Fish Physiol Biochem (2022) 48:1571–1586
https://doi.org/10.1007/s10695-022-01127-8

Lipid-related metabolism during zebrafish embryogenesis under unbalanced copper homeostasis

ChangShun Li · You Wu · HaoTian Li · Hai Wang · Jing-Xia Liu

Received: 11 May 2022 / Accepted: 17 September 2022 / Published online: 26 September 2022

Abstract Copper (Cu) is an essential trace element, playing an important role in lipid metabolism, and its transporters ATP7A and ATP7B, as Cu-transporting P-type ATPases, are involved in maintaining the Cu homeostasis in cells. Numerous studies in mammals have shown that Cu homeostasis and lipid metabolism are closely related, but studies on the link between the effects of excess Cu, ATP7A, and ATP7B on lipid metabolism during vertebrate embryogenesis are scarce. In this study, zebrafish disease models with Cu overload and ATP7A and ATP7B inactivation, respectively, were used to study the lipid metabolism-related differentially expressed genes (DEGs) which were enriched in the models. The dynamic and spatiotemporal expressions of the DEGs in WTs, *atp7a*$^{-/-}$, and *atp7b*$^{-/-}$ mutants with or without Cu stress were unveiled in this study and they mostly distributed in brain at 24 hpf then in liver and intestine at 96 hpf, suggesting their potential roles in lipid and glycogen metabolism to apply energy for normal development in zebrafish. Meanwhile, the correlation analysis for the DEGs among the three groups unveiled that most of the DEGs were involved in the glyceride metabolism pathway. This is the first report to establish the relationship between *atp7a* and *atp7b* with Cu-stimulated intestinal and liver lipid metabolism during fish embryogenesis, and this study will provide a theoretical basis for fish embryonic development and lipid metabolism disorders under unbalanced copper homeostasis.

Keywords Cu · *atp7a*$^{-/-}$ · *atp7b*$^{-/-}$ · Lipid metabolism · Glyceride metabolism

Introduction

As an essential trace element for living organisms, Copper (Cu) is a cofactor for various enzymes and plays important roles in many physiological activities, such as cellular respiration, lipid metabolism, and iron ion uptake (Festa and Thiele 2011). Disruption of intracellular Cu homeostasis contributes to developmental abnormalities and metabolic diseases (Llanos and Mercer 2002), such as Alzheimer's disease (Brewer et al. 2010), celiac disease (Halfdanarson et al. 2009), and fatty liver (Morrell et al. 2017).

ChangShun Li and You Wu are the first authors of the paper.

Supplementary Information The online version contains supplementary material available at https://doi.org/10.1007/s10695-022-01127-8.

C. Li · Y. Wu · H. Li · J.-X. Liu (✉)
College of Fisheries, Key Laboratory of Freshwater Animal Breeding, Ministry of Agriculture, Huazhong Agricultural University, Wuhan 430070, China
e-mail: ichliu@mail.hzau.edu.cn

H. Wang
Wuhan Zhihuiyuan Environmental Protection Technology, Co., Ltd, Wuhan 430070, China

Cu exists in many forms in natural water and distributes in various components of aquatic ecosystem; among them, free Cu^{2+} is generally considered to be the main ion form of Cu toxicity to aquatic organisms (Tai et al. 2019). Nowadays, with the widespread use of Cu sulfate as an algicide and feed addition in aquaculture, the pollution of heavy metal Cu to the aquatic environment and fish has gradually increased (Antonio Guardiola et al. 2012; Chen et al. 2019). It is reported that the average Cu concentration in unpolluted rivers is 0.25~2 μg/L, and the concentration of Cu in polluted water usually rises dozens or even hundreds of times (Makokha et al. 2016). Excessive Cu destroys water ecology (Fortin et al. 2010), and can accumulate in aquatic organisms and then bioaccumulates in the human body through food chain to cause tissues and organ damages (Brewer 2015; Morrell et al. 2017).

Studies have found that Cu regulates lipolysis (Krishnamoorthy et al. 2016) and activates cholesterol-producing genes in macrophages (Svensson et al, 2003). In addition, studies have unveiled that Cu exposure induces differentially expressed lipid metabolism genes in juvenile yellow catfish in liver and visceral adipose (Chen et al. 2012), and the authors unveil that SREBP-1 and LXRa pathways mediate Cu-induced hepatic lipid metabolism dysfunction in fish (Pan et al. 2018). In this study, based on transcriptome data, differentially expressed genes (DEGs) associated with lipid metabolism were found in Cu-stressed zebrafish embryos, and zebrafish mutant embryos (*atp7a*$^{-/-}$ and *atp7b*$^{-/-}$) with deletion of Cu-transporting P-type ATPases, ATP7A and ATP7B, respectively, and the transcriptional level and distribution of the DEGs during embryogenesis were tested further in this study.

The important Cu-transporting P-type ATPases, ATP7A and ATP7B, are involved in the synthesis of intracellular Cu enzymes and maintain Cu homeostasis in vivo (La Fontaine and Mercer 2007; Linder et al. 1998; Oehrvik et al 2014). ATP7A, localized in intestinal epithelial cells, mainly transports intestinal Cu to the circulatory system (Loennerdal, 2008; Ravia et al. 2005). Deficiency of ATP7A results in massive accumulation of Cu in the intestine (Zhao et al. 2020a, 2020b), inducing intestinal lipid imbalance and disrupting Cu homeostasis in the body (Tao et al. 2019). Meanwhile, the essential function of ATP7B is to promote the excretion of hepatic Cu (Pfeil and Lynn 1999), and the functional mutation of ATP7B leads to the accumulation of Cu in the liver and the resulting in Wilson's disease (WD) (Mi et al. 2020) with the main symptoms of liver damage and cirrhosis (Ala et al. 2007; Pfeil and Lynn 1999). However, rare studies have examined the relationship between the effects of Cu overload on lipid metabolism during zebrafish embryogenesis and examined the roles of Cu-transporting ATPases, ATP7A and ATP7B, in Cu overload–induced lipid dysmetabolism. Our previous studies have revealed that nano-Cu (CuNPs) and ions (Cu^{2+}) could induce intestinal developmental defects by triggering endoplasmic reticulum (ER) stress and reactive oxygen species (ROS) stress (Zhao et al. 2020b). In this study, the dynamic expressions of the differentially expressed lipid metabolism-related genes in Cu-stressed zebrafish and in *atp7a*$^{-/-}$ and *atp7b*$^{-/-}$ mutants with and without Cu stresses were tested, which mainly distributed in liver and intestine during embryogenesis. The purpose of this study was to investigate the effects of Cu stress and functional loss of Cu transporter ATPases ATP7A and ATP7B on lipid metabolism and to verify the integrated functions of Cu transporters ATP7A and ATP7B on lipid metabolism in body with Cu overload.

Materials and methods

Maintenance of zebrafish stocks and embryo and larvae collection

According to standard procedures (provided by China Zebrafish Resource Center, http://www.zfish.cn/), the AB wild type (WT), *atp7a* and *atp7b* homozygous (*atp7a*$^{-/-}$, *atp7b*$^{-/-}$) mutant adult zebrafish (Zhang et al. 2020; Zhao et al. 2020a, 2020b) were cultured in a circulating filtration system (28 ± 0.5 °C, 14:10 h light/dark) and fed three times per day (morning at 9:00 A.M.; afternoon at 3:00 P.M.; night at 9:00 P.M.) with *Artemia salina* hatched from commercial *Artemia salina* eggs (Tianjin Fengnian Aquaculture Co., Ltd. China). Male and female zebrafish were kept separately until mating and spawning. After natural spawning, embryos were pooled and washed, and then the fertilized embryos and larvae were collected under a dissection microscope (SMZ168; Motic, China). Natural spawning eggs were obtained and maintained in a 28.5 °C incubator. The ages of the

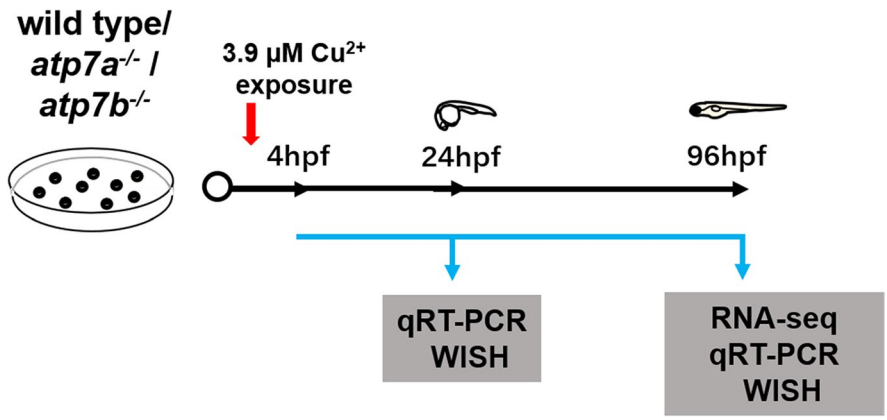

Scheme 1 Embryos with and without Cu stimulation collected separately at 24 hpf or 96 hpf for different assays

embryos and larvae were expressed in hours post-fertilization (hpf) or days post-fertilization (dpf).

Atp7a and atp7b homozygous mutant construction

Atp7a$^{-/-}$ and *atp7b*$^{-/-}$ homozygous mutants were constructed by CRISPR/Cas9 technology in our laboratory recently, and *atp7a*$^{-/-}$ mutants were used to test its roles in retinal and intestinal developmental defects induced by Cu overload recently (Zhao et al. 2020a, 2020b), and *atp7b*$^{-/-}$ mutants were used to test its roles in axon and myelin developmental defects induced by Cu overload (Zhang et al. 2020). The transcriptional profiles of *atp7a*$^{-/-}$ and *atp7b*$^{-/-}$ homozygous mutated larvae were presented in other two manuscripts which are under reviewing process. In the manuscript, we focused on transcriptional data in ion transporter, angiogenesis, ATPase activities, and in neurexin family protein binding in the *atp7a*$^{-/-}$ mutants with and without Cu stress, and focused on transcriptional data in sensory perception of light stimulus, visual perception, lens development in camera-type eye, etc. in *atp7b*$^{-/-}$ mutants with and without Cu stress.

Cu^{2+} exposure and measurement

In this study, 0.25 mg/L Cu^{2+} (3.9 μM) (stock solution was prepared with ultrapure water) was used to stress the zebrafish embryos as reported previously (Zhang et al. 2020, 2015).Six groups, WT (wild type), WT + Cu (wild type stressed with Cu), *atp7a*$^{-/-}$, and *atp7a*$^{-/-}$ + Cu (*atp7a*$^{-/-}$ stressed with Cu), *atp7b*$^{-/-}$, and *atp7b*$^{-/-}$ + Cu (*atp7a*$^{-/-}$ stressed with Cu), were performed in this study. Each group was replicated three times. The collected embryos and larvae were staged by morphological features (Kimmel et al. 1995). The embryos with and without Cu stimulation were collected separately at 24 hpf or 96 hpf for different assays as shown in Scheme 1. Cu^{2+} mediums prepared with ultrapure water or fish system circulating water were collected at 0 h (at 0 h the embryos were added), 24 h, and 96 h with or without embryos, and the contents of Cu^{2+} in the solution were determined by atomic absorption spectroscopy (Varian, AA240FS). Standard reference materials (GSB 04–1725-2004, acquired from Chinese Academy of Measurement Science) were used to create a standard curve to measure and estimate the Cu^{2+} content in the aforementioned samples. Three parallel experiments were performed and the results were calculated and shown in Table 1.

Analysis of differentially expressed lipid metabolism-related genes based on RNA-Seq data

atp7a$^{-/-}$, *atp7b*$^{-/-}$, and WT embryos with or without Cu stress were collected at 96 hpf, respectively, and were used for RNA extraction and RNA-Sequencing (RNA-Seq). Transcriptome in Cu-stressed WT zebrafish has been reported recently (Zhang et al. 2020, 2018; Zhao et al. 2020a, 2020b), and details of transcriptome of *atp7a*$^{-/-}$ and *atp7b*$^{-/-}$, respectively, have been presented in the two aforementioned manuscripts under reviewing process. For the identification of DEGs, data from two replicates were normalized and the *P* values were calculated as reports performed. Fold change (FC) analysis using normalized read counts was determined for each gene by dividing the normalized intensity values in

Table 1 Analysis of Cu^{2+} concentrations (mg/L)

Group		Concentrations (mg/L)	RSDs (%)
Ultrapure water	0 h	0.005	3.2
	24 h	0.007	4.7
	96 h	0.002	3.4
Fish system water	0 h	0.012	4.7
	24 h	0.009	8.5
	96 h	0.014	7.6
Ultrapure water + Cu^{2+} (without embryos)	0 h	0.258	1.8
	24 h	0.253	1.1
	96 h	0.254	3.1
Fish system water + Cu^{2+} (without embryos)	0 h	0.261	2.5
	24 h	0.265	1.4
	96 h	0.255	2.7
Ultrapure water + Cu^{2+} (with embryos)	0 h	0.248	4.2
	24 h	0.237	6.8
	96 h	0.217	1.9
Fish system water + Cu^{2+} (with embryos)	0 h	0.261	4.1
	24 h	0.238	2.8
	96 h	0.222	3.2

the Cu-stressed, or *atp7a*$^{-/-}$, or *atp7b*$^{-/-}$ libraries by values in the WT libraries, respectively. Genes with significant alterations due to *atp7a* or *atp7b* mutation or Cu stress (adjusted $P < 0.05$) were defined as differentially expressed genes (DEGs) and subjected to functional annotation analysis.

In this study, based on the RNA-Seq data, we focused on differentially expressed lipid metabolism-related genes which unveiled from *atp7a*$^{-/-}$, *atp7b*$^{-/-}$ mutants or from Cu-stressed WTs. We tested their dynamic expressions during embryogenesis in WTs and the mutants with and without Cu stresses in this study.

qRT-PCR

Briefly, 30–50 embryos/sample were collected at 24 hpf and 96 hpf, respectively, for RNA extraction using 1 mL Trizol reagent (Invitrogen) to detect the transcriptional expression of the representative genes in this study. cDNA was synthesized using a M-MLV Reverse-Transcript Kit (Applied Biological Materials Inc., BC, Canada). Quantitative PCR was performed using iQ SYBR Green Super Mix (Bio-Rad Laboratories, USA) in a CFX Connect Real-Time PCR Detection System (Bio-Rad Laboratories, USA). In this study, the genes used for qRT-PCR assays include *hmgcs1*, *cel.2*, *elovl2*, *gck*, *gla*, *gsr*, *st3gal5*, *elovl8b*, *akr1a1b*, *hmgcll1*, *elovl4b*, *lss*, *apoa4b.1*, and *dgat1a*. The gene full names and the sequences of qRT-PCR primers are listed in Table S1. All of the experiments were performed in at least triple duplicates. Differences were calculated according to the $2^{-\Delta\Delta Ct}$ comparative quantization method using 18 s or β-actin as an internal, and the data were analyzed with one-way analysis of variance (ANOVA) and post hoc Tukey's test. We found that the results of using 18 s as an internal control were consistent with the results of using β-actin; thus, we presented one series of data for each experiment for the RT-PCR assays in this study.

WISH

In order to study the distribution and expression level of the tested genes in the whole embryo during embryogenesis, specific DIG-labeled antisense RNA probes were synthesized using T7 or Sp6 in vitro transcription polymerase and DIG RNA labeling kit (Roche Molecular Biochemicals, Germany), performing as reported in our previous studies (Liu et al. 2013; Zhang et al. 2015). The DEGs used for probe synthesis are all related to lipid metabolism such as *hmgcs1*, *cel.2*, *elovl2*, *gck*, *gla*, *gsr*, *st3gal5*, *elovl8b*, *akr1a1b*, *hmgcll1*, *elovl4b*, *lss*, *apoa4b.1*, and *dgat1a*. The gene full names and the primers used for amplifying whole-mount in situ hybridization (WISH) probes are listed in Table S2. The antibody used to

detect in situ hybridization was Anti-Digoxigenin-AP Fab fragments (Roche Molecular Biochemicals, Germany). The probes' positive signals were purple and were specifically distributed in the labeling cells of embryos. The relative intensity of purple signals indicated the transcriptional level of the labeling gene. Embryos were observed and photographed under a stereoscopic microscope (Leica M205FA, Germany). This technique allowed us to quantify the specific distribution and expression level of the tested gene in the whole-mount embryos. Compared to the signals in the control, embryos with weaker purple staining were defined as embryos with reduced gene expression, and the percentage of embryos with reduced gene transcripts was calculated using the following method, $P = N_{reduced}/N_{total}$, where $N_{reduced}$ was the number of embryos displaying reduced probe staining and N_{total} was the total number of embryos used for probe staining in each assay. A minimum of 20 embryos from each treatment and the control group were used for whole-mount in situ hybridization in this study, and all of the experiments were performed in at least two or triple duplicates**.**

Statistical analysis

The qRT-PCR results were performed using one-way ANOVA and post-mortem Turkish Social Science Statistical Package Test (SPSS) 19.0 software (SPSS, Chicago, Illinois, USA). Statistical data of the signal area for WISH data in different samples were analyzed using *t* test by GraphPad Prism 7.00 software as we performed previously (Zhang et al. 2020), and WISH data between different groups were comprised using hypergeometric distribution in R-console software (https://www.r-project.org/). Data were represented as mean ± SD, $*P < 0.05$, $**P < 0.01$, $***P < 0.001$.

Results

Measurement of Cu^{2+} solution concentration

The experimental results (Table 1) showed that the concentrations of Cu solutions prepared by fish system circulating water were slightly higher than that of Cu solutions prepared by ultrapure water, and the Cu solutions maintained a concentration of about 0.25 mg/L at 0 h, 24 h, and 96 h without embryos, which is consistent with the report that the concentration of heavy metal ions in water was relatively stable (Shan et al. 2010). In the presence of embryos, the Cu concentration in solutions decreased slightly at 24 h and 96 h, suggesting the reduced Cu in solutions might be absorbed by the embryos. Meanwhile, the relative standard deviations (RSDs) among the samples were less than 10% in this study.

Cu alters the expression of genes associated with lipid metabolism in zebrafish embryos

Recently, we detected the transcription profiles of WT, WT + Cu, *atp7a*$^{-/-}$, and *atp7a*$^{-/-}$ + Cu, *atp7b*$^{-/-}$, and *atp7b*$^{-/-}$ + Cu zebrafish larvae at 96 hpf via RNA-Seq. The general transcription profiles in WTs have been reported recently (Zhang et al. 2020, 2018; Zhao et al. 2020a, 2020b), and the general transcription profiles in *atp7a*$^{-/-}$ and *atp7b*$^{-/-}$ mutants with or without Cu stress were analyzed and presented in the aforementioned manuscripts (under reviewing), respectively. Based on the transcriptional profiles, we focused on genes related to lipid metabolism in WT, *atp7a*$^{-/-}$, and *atp7b*$^{-/-}$ mutated larvae with or without Cu stress in this study. In WT embryos stressed with Cu at 96 hpf, GO analysis for DEGs showed that they were significantly enriched in lipid metabolism-related entries (Fig. 1A; Table S3). Cluster analysis was performed on DEGs related with lipid metabolism, such as genes *hmgcs1*, *cel.2*, *elovl2*, and *gck* (Fig. 1B). qRT-PCR further showed the differential expressions of lipid metabolism-related DEGs between Cu-stressed and WT embryos at 24 hpf and 96 hpf, and the qRT-PCR results at 96 hpf showed the down-regulated expression of genes *hmgcs1*, *cel.2*, and *elovl2* but up-regulated expression of *gck*, which were consistent with the transcriptome data. Meanwhile, genes *hmgcs1*, *cel.2*, and *elovl2* exhibited up-regulated expression in Cu-stressed embryos at 24 hpf (Fig. 1C).

In addition, WISH showed that the expressions of *hmgcs1*, *elovl2*, *cel.2*, and *gck* had different spatiotemporal specificities. In zebrafish embryos at 24 hpf, these four genes were significantly expressed mainly in the head region, and there was no significant change in *cel.2* while *hmgcs1* and *elovl2* were reduced but *gck* increased at 24 hpf (Fig. 1D). In zebrafish larvae at 96 hpf, *hmgcs1*, *elovl2*, and

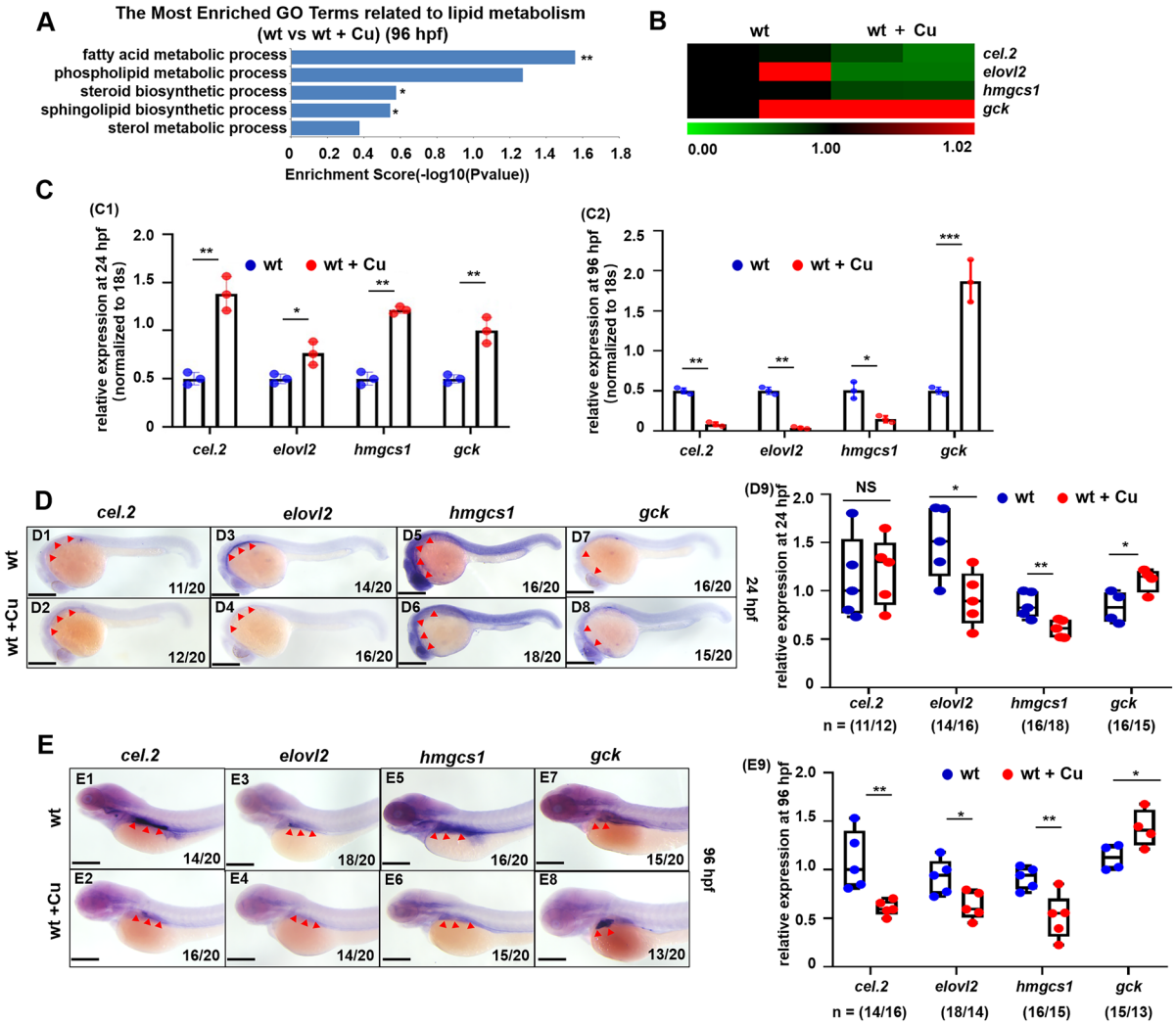

Fig. 1 Transcriptional profiling in WT vs. WT + Cu and expression of lipid metabolism-related genes in WT and Cu-stressed WT. (**A**) GO term analysis of the DEGs in 96-hpf WT vs. WT + Cu. (**B**) Clustering analysis of lipid metabolism-related genes in WT vs. WT + Cu. (**C**) qRT-PCR analysis of lipid metabolism-related genes in embryos from WT and Cu-stressed WT groups at 24 hpf and 96 hpf. (**D**) WISH analysis of the expression of *cel.2* (D1, D2), *elovl2* (D3, D4), *hmgcs1* (D5, D6), *gck* (D7, D8) in embryos from WT and Cu-stressed WT groups at 24 hpf. (D9) The relative expression of *cel.2*, *elovl2*, *hmgcs1*, *gck* at 24 hpf. (**E**) WISH analysis of the expression of *cel.2* (E1, E2), *elovl2* (E3, E4), *hmgcs1* (E5, E6), *gck* (E7, E8) in embryos from WT and Cu-stressed WT groups at 96 hpf. (E9) The relative expression of *cel.2*, *elovl2*, *hmgcs1*, *gck* at 96 hpf. D1–D8 and E1–E8, lateral view, anterior to the left, and scale bar: D1–D8 and E1–E8, 100 μm. $^{*}P < 0.05$, $^{**}P < 0.01$, $^{***}P < 0.001$. NS, not significant

cel.2 were mainly expressed in the gut, and *gck* was mainly expressed in the liver (Fig. 1E), and *hmgcs1*, *elovl2*, and *cel.2* were reduced while *gck* increased, which was consistent with the aforementioned qRT-PCR results and the transcriptome data.

Expression of lipid metabolism-related genes in atp7a$^{-/-}$ mutants with and without Cu stress

DEGs in *atp7a*$^{-/-}$ embryos at 96 hpf were screened, and significantly enriched GO terms such as cholesterol metabolic process and steroid and lipid

biosynthetic process were followed with interest in this study (Fig. 2A; Table S4). The cluster analysis of lipid metabolism-related DEGs such as *gla*, *gsr*, *st3gal5*, and *elovl8b* in *atp7a*$^{-/-}$ mutants was performed (Fig. 2B). The results of qRT-PCR showed that expressions of *gla*, *gsr*, *st3gal5*, and *akr1a1b* were increased while *elovl8b* reduced in *atp7a*$^{-/-}$ mutants at 96 hpf (Fig. 2C2), which was consistent with the transcriptome data. Meanwhile, the expression of *gla*, *gsr*, *st3gal5*, and *akr1a1b* exhibited increased expression at 24 hpf (Fig. 2C1). WISH results were consistent with qRT-PCR and transcriptome results at 96 hpf (Fig. 2D1–D11). Next, we detected expressions of DEGs unveiled in Cu-stressed zebrafish larvae which

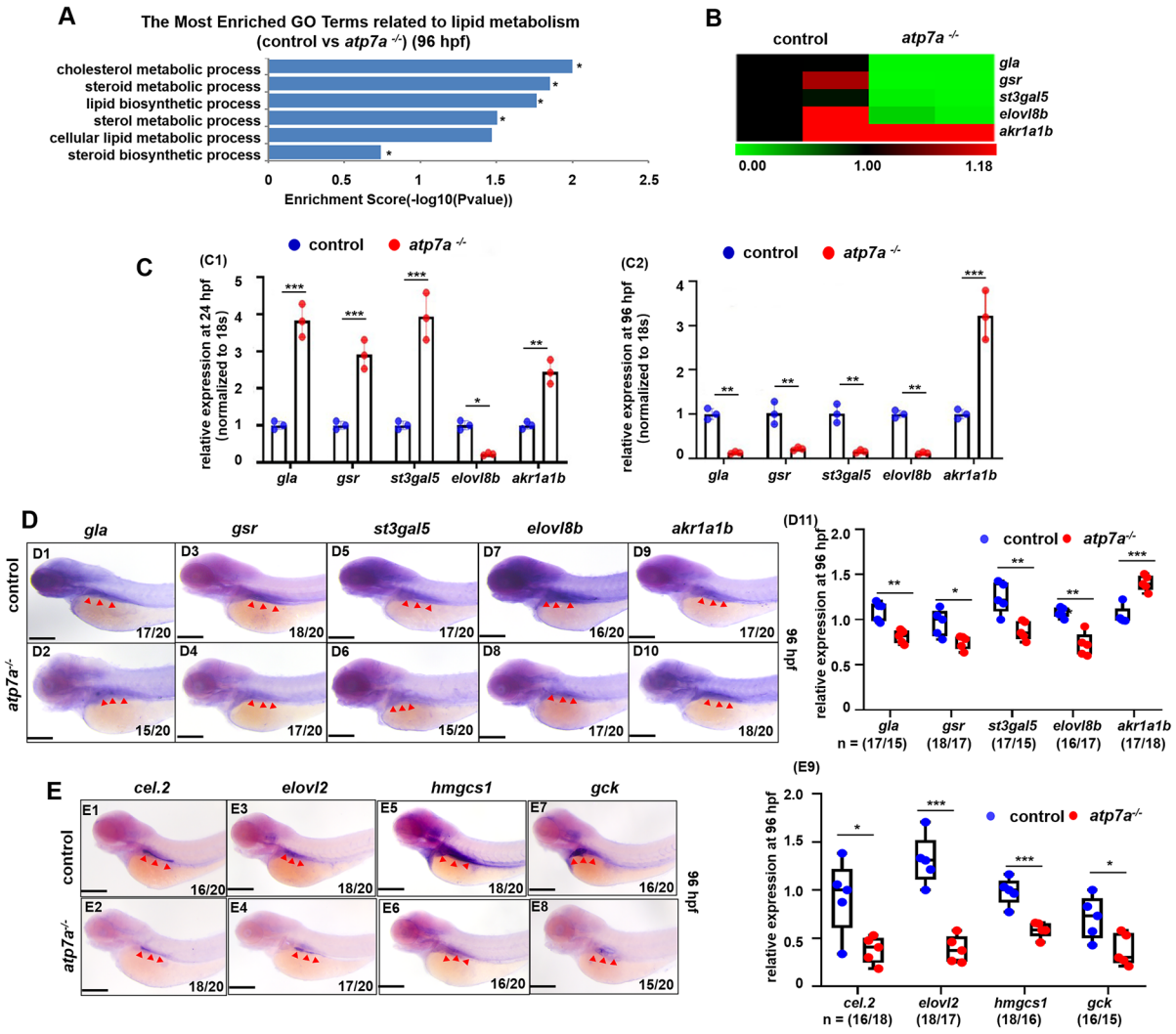

Fig. 2 Transcriptional profiling in WT vs. *atp7a*$^{-/-}$ and expression of lipid metabolism-related genes in WT and *atp7a*$^{-/-}$. (**A**) GO term analysis of the DEGs in 96-hpf WT vs. *atp7a*$^{-/-}$. (**B**) Clustering analysis of lipid metabolism-related genes in WT vs. *atp7a*$^{-/-}$. (**C**) qRT-PCR analysis of lipid metabolism-related genes in embryos from WT and *atp7a*$^{-/-}$ groups at 24 hpf and 96 hpf. (**D**) WISH analysis of the expression of *gla* (D1, D2); *gsr* (D3, D4); *st3gal5* (D5, D6); *elovl8b* (D7, D8); *akr1a1b* (D9, D10) in embryos from WT and *atp7a*$^{-/-}$ groups at 96 hpf. (D11) The relative expression of *gla*, *gsr*, *st3gal5*, *elovl8b*, *akr1a1b* at 96 hpf. (E) WISH analysis of the expression of *cel.2* (E1, E2); *elovl2* (E3, E4); *hmgcs1* (E5, E6); *gck* (E7, E8) in embryos from WT and *atp7a*$^{-/-}$ groups at 96 hpf. (E9) The relative expression of *cel.2*, *elovl2*, *hmgcs1*, *gck* at 96 hpf. D1–D10 and E1–E8, lateral view, anterior to the left, and scale bar: D1–D10 and E1–E8, 100 μm. *$P < 0.05$, **$P < 0.01$, ***$P < 0.001$. NS, not significant

were related to lipid metabolism in *atp7a*$^{-/-}$ mutants, to explore whether the deficiency of *atp7a* function would also affect the expression of these genes in the mutants. WISH results showed that *hmgcs1*, *elovl2*, *cel.2*, and *gck* genes were significantly down-regulated in *atp7a*$^{-/-}$ mutants (Fig. 2E1–E9).

We checked the transcriptional data in *atp7a*$^{-/-}$ with and without Cu stress, and DEGs related with lipid metabolism in *atp7a*$^{-/-}$ embryos after Cu stress at 96 hpf were screened. Significantly enriched GO terms such as adipocytokine signaling pathway and steroid hormone biosynthesis were followed with interest in this study (Fig. 3A; Table S5). The cluster analysis of lipid metabolism-related DEGs such as *cyp1a*, *cyp3a65*, *pnp5a*, *g6pca.2*, and *pck1* in *atp7a*$^{-/-}$ mutants after Cu stress was performed (Fig. 3B). Next, we tested the expressions of the aforementioned lipid metabolism related DEGs in *atp7a*$^{-/-}$ mutants stressed with Cu at 96 hpf via WISH assays. Expression of lipid metabolism-related DEGs unveiled in *atp7a*$^{-/-}$ mutant had no significant change in *atp7a*$^{-/-}$ mutants stressed with Cu at 96 hpf (Fig. 3BC1–C11). Meanwhile, the expression levels of genes *elovl2* and *cel.2* were still significantly down-regulated with no significant difference in the expressions of genes *hmgcs1* and *gck* in *atp7a*$^{-/-}$ mutants with Cu stress, which are DEGs unveiled in Cu-stressed larvae (Fig. 3D1–D9).

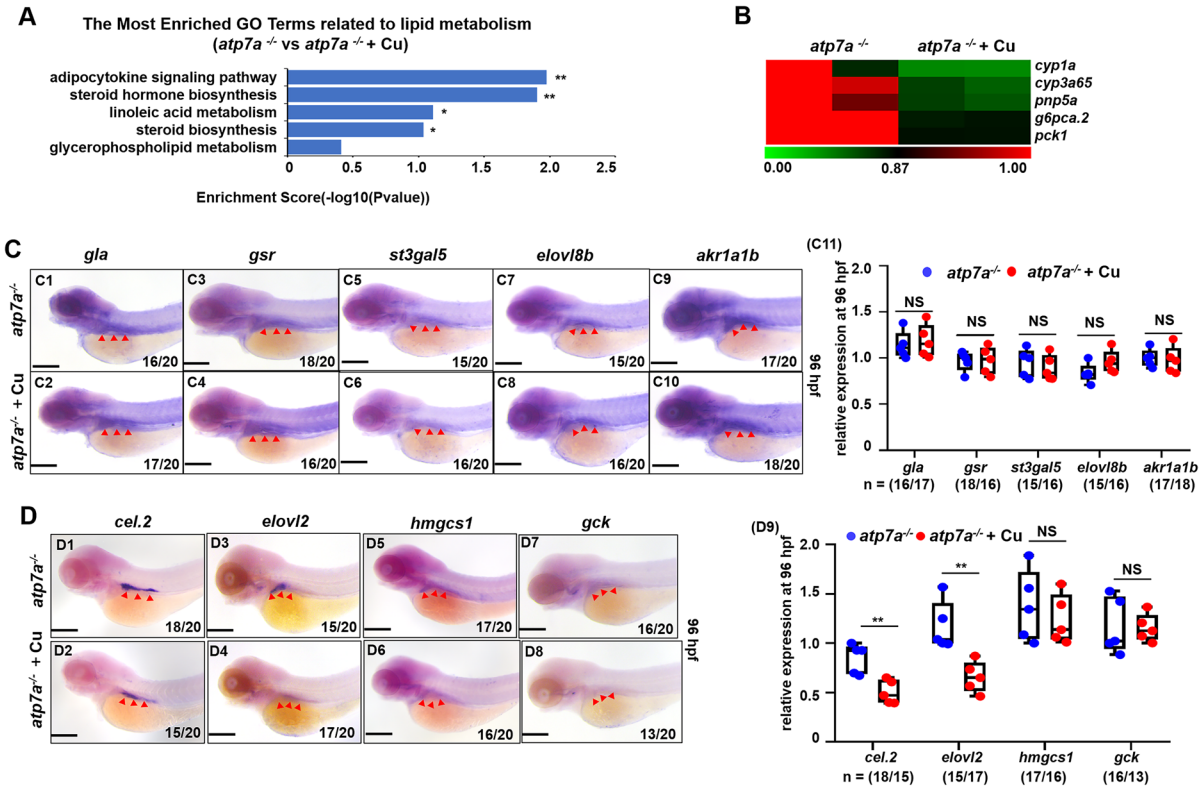

Fig. 3 Transcriptional profiling in *atp7a*$^{-/-}$ vs. *atp7a*$^{-/-}$ +Cu and expression of lipid metabolism-related genes in *atp7a*$^{-/-}$ and Cu-stressed *atp7a*$^{-/-}$. (**A**) GO term analysis of the DEGs in 96-hpf *atp7a*$^{-/-}$ vs. *atp7a*$^{-/-}$ +Cu. (**B**) Clustering analysis of lipid metabolism-related genes in *atp7a*$^{-/-}$ vs. *atp7a*$^{-/-}$ +Cu. (**C**) WISH analysis of the expression of *gla* (C1, C2); *gsr* (C3, C4); *st3gal5* (C5, C6); *elovl8b* (C7, C8); *akr1a1b* (C9, C10) in embryos from *atp7a*$^{-/-}$ and Cu-stressed *atp7a*$^{-/-}$ groups at 96 hpf. (C11) The relative expression of *gla*, *gsr*, *st3gal5*, *elovl8b*, *akr1a1b* at 96 hpf. (**D**) WISH analysis of the expression of *cel.2* (D1, D2); *elovl2* (D3, D4); *hmgcs1* (D5, D6); *gck* (D7, D8) in embryos from *atp7a*$^{-/-}$ and Cu-stressed *atp7a*$^{-/-}$ groups at 96 hpf. (D9) The relative expression of *cel.2*, *elovl2*, *hmgcs1*, *gck* at 96 hpf. C1–C10 and D1–D8, lateral view, anterior to the left, and scale bar: C1–C10 and D1–D8, 100 μm. *$P<0.05$, **$P<0.01$, ***$P<0.001$. NS, not significant

Expression of lipid metabolism-related genes in atp7b$^{-/-}$ mutants with and without Cu stress

DEGs in *atp7b*$^{-/-}$ embryos at 96 hpf were screened and significantly enriched GO terms such as cholesterol biosynthetic process and steroid esterification were followed with interest in this study (Fig. 4A; Table S6). The cluster analysis of lipid metabolism-related DEGs such as *hmgcll1*, *lss*, *elovl4b*, *apoa4b.1*, and *dgat1a* in *atp7b*$^{-/-}$ mutants was performed (Fig. 4B). The results of qRT-PCR were consistent with the transcriptional profiles, with genes *hmgcll1* and *lss* down-regulated while genes *apoa4b.1* and *dgat1a* up-regulated, and *elovl4b* no significant change (Fig. 4C). Furthermore, WISH results in *atp7b*$^{-/-}$ embryos at 96 hpf were consistent with transcriptome analysis results (Fig. 4D1–D11). Next, we detected expressions of DEGs unveiled in Cu-stressed zebrafish larvae which were related to lipid metabolism in *atp7b*$^{-/-}$ mutants, to explore

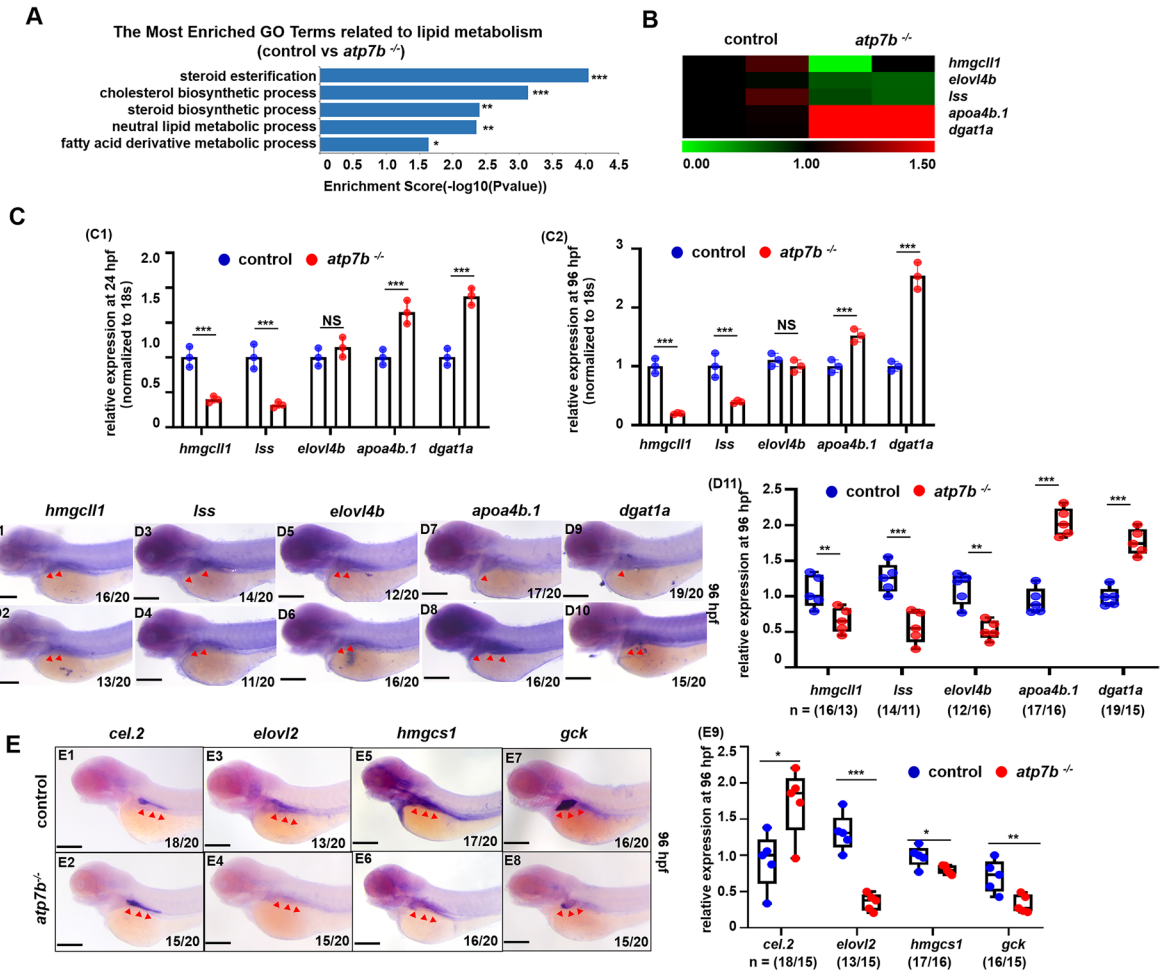

Fig. 4 Transcriptional profiling in WT vs *atp7b*$^{-/-}$ and expression of lipid metabolism-related genes in WT and *atp7b*$^{-/-}$. (**A**) GO term analysis of the DEGs in 96-hpf WT vs. *atp7b*$^{-/-}$. (**B**) Clustering analysis of lipid metabolism-related genes in WT vs. *atp7b*$^{-/-}$. (**C**) qRT-PCR analysis of lipid metabolism-related genes in embryos from WT and *atp7b*$^{-/-}$ groups at 24 hpf and 96 hpf. (**D**) WISH analysis of the expression of *hmgcll1* (D1, D2); *lss* (D3, D4); *elovl4b* (D5, D6); *apoa4b.1* (D7, D8); *dgat1a* (D9, D10) in embryos from WT and *atp7b*$^{-/-}$ groups at 96 hpf. (D11) The relative expression of *hmgcll1*, *lss*, *elovl4b*, *apoa4b.1*, *dgat1a* at 96 hpf. (**E**) WISH analysis of the expression of *cel.2* (E1, E2); *elovl2* (E3, E4); *hmgcs1* (E5, E6); *gck* (E7, E8) in embryos from WT and *atp7b*$^{-/-}$ groups at 96 hpf. (E9) The relative expression of *cel.2*, *elovl2*, *hmgcs1*, *gck* at 96 hpf. D1–D10 and E1–E8, lateral view, anterior to the left, and scale bar: D1–D10 and E1–E8, 100 μm. *$P<0.05$, **$P<0.01$, ***$P<0.001$. NS, not significant

whether the deficiency of *atp7b* function would also affect the expression of these genes in the mutants. WISH results showed that *hmgcs1*, *elovl2*, and *gck* genes were significantly down-regulated and *cel.2* was significantly up-regulated in *atp7b*$^{-/-}$ mutants (Fig. 4E1–E9).

Next, we checked the transcriptional data in *atp7b*$^{-/-}$ with and without Cu stress. DEGs in lipid metabolism in *atp7b*$^{-/-}$ embryos after Cu stress at 96 hpf were screened. Significantly enriched GO terms such as cholesterol homeostasis and unsaturated fatty acid metabolic process were followed with interest in this study (Fig. 5A; Table S7). The cluster analysis of lipid metabolism-related DEGs such as *dgat2*, *elovl1b*, *hk2*, *hsd17b12a*, *elovl1a*, and *elovl7b* in *atp7b*$^{-/-}$ mutants after Cu stress was performed (Fig. 5B). Next, we tested expressions of the aforementioned lipid metabolism-related DEGs in *atp7b*$^{-/-}$ mutants stressed with Cu at 96 hpf via WISH assays. For lipid metabolism DEGs unveiled in *atp7b*$^{-/-}$ mutants, except for the slight down-regulation of *lss* expression in *atp7b*$^{-/-}$ mutants stressed with Cu, the other four genes did not change significantly after Cu stress (Fig. 5C1–C10). However, for lipid metabolism-related DEGs unveiled in *atp7b*$^{-/-}$ mutants stressed with Cu, the expression levels of genes *hmgcs1*, *elovl2*, *cel.2*, and *gck* were all found to be significantly down-regulated further (Fig. 5D1–D9).

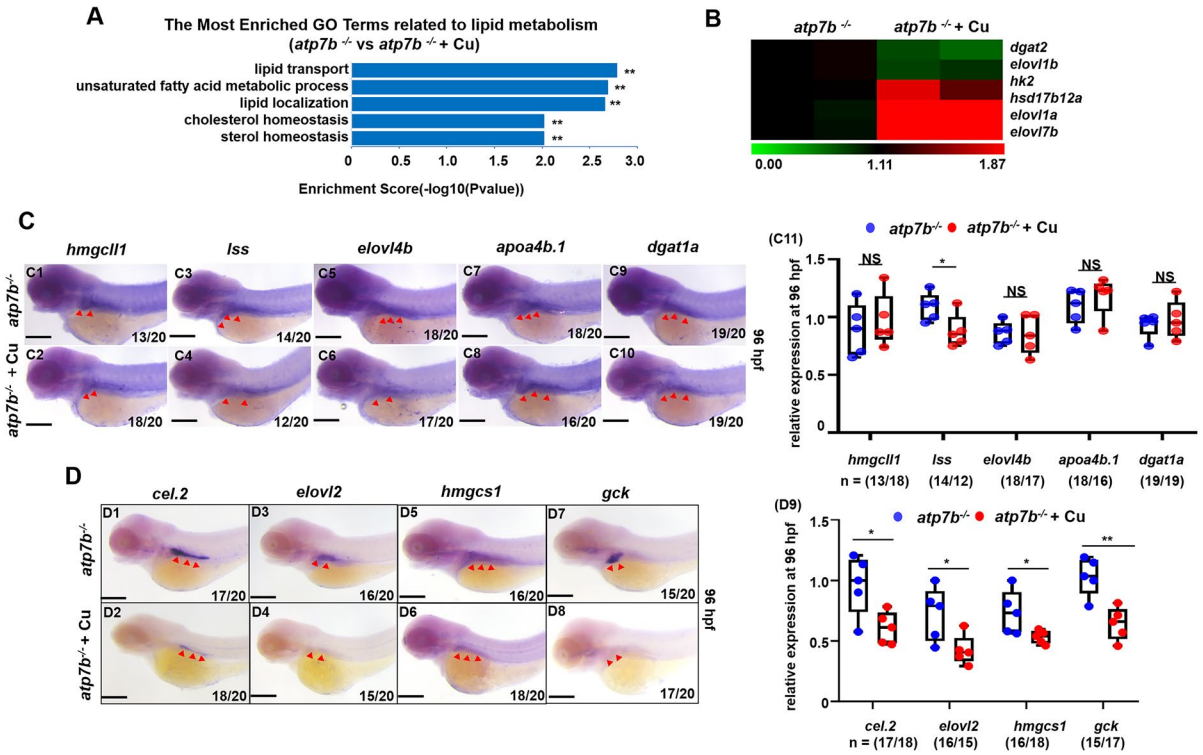

Fig. 5 Transcriptional profiling in *atp7b*$^{-/-}$ vs. *atp7b*$^{-/-}$ +Cu and expression of lipid metabolism-related genes in *atp7b*$^{-/-}$ and Cu-stressed *atp7b*$^{-/-}$. (**A**) GO term analysis of the DEGs in 96-hpf *atp7b*$^{-/-}$ vs. *atp7b*$^{-/-}$ +Cu. (**B**) Clustering analysis of lipid metabolism-related genes in *atp7b*$^{-/-}$ vs. *atp7b*$^{-/-}$ +Cu. (**C**) WISH analysis of the expression of *hmgcll1* (C1, C2); *lss* (C3, C4); *elovl4b* (C5, C6); *apoa4b.1* (C7, C8); *dgat1a* (C9, C10) in embryos from *atp7b*$^{-/-}$ and Cu-stressed *atp7b*$^{-/-}$ groups at 96 hpf. (C11) The relative expression of *hmgcll1*, *lss*, *elovl4b*, *apoa4b.1*, *dgat1a* at 96 hpf. (**D**) WISH analysis of the expression of *cel.2* (D1, D2); *elovl2* (D3, D4); *hmgcs1* (D5, D6); *gck* (D7, D8) in embryos from *atp7b*$^{-/-}$ and Cu-stressed *atp7b*$^{-/-}$ groups at 96 hpf. (D9) The relative expression of *cel.2*, *elovl2*, *hmgcs1*, *gck* at 96 hpf. C1–C10 and D1–D8, lateral view, anterior to the left, and scale bar: C1–C10 and D1–D8, 100 μm. *$P<0.05$, **$P<0.01$, ***$P<0.001$. NS, not significant

Altered glyceride metabolism-related genes in zebrafish embryos with unbalanced Cu hemostasis

The correlation between lipid metabolism-related DEGs of WT + Cu, *atp7a*$^{-/-}$, *atp7b*$^{-/-}$, *atp7a*$^{-/-}$ + Cu, and *atp7b*$^{-/-}$ + Cu was established by KEGG pathway analysis. It was found that most of the DEGs were involved in the glyceride metabolism pathway (Fig. 6). Among them, *elovl2*, *elovl1b*, *elovl4b*, *elovl7b*, *elovl8b*, *elovl1a*, and *hsd17b12a* are genes for long-chain fatty acid synthesis, which was an important component of glycerides (Liu et al. 2020; Logan et al. 2014; Pauter et al. 2014; Sassa et al. 2013). Furthermore, *hmgcs1* and *hmgcll1* are involved in the synthesis of cholesterol, and *cel.2*, *dgat2*, and *dgat1a* are regulators of steroid biosynthesis. Alterations in these genes can directly or indirectly affect glyceride metabolism.

Discussion

In this study, we found that lipid and glyceride metabolism-related DEGs were enriched via screening the aforementioned RNA-Seq data, then the dynamic and spatiotemporal expressions of the DEGs in WTs, *atp7a*$^{-/-}$, and *atp7b*$^{-/-}$ mutants with or without Cu stress were unveiled. This correlation analysis for the DEGs unveiled that most of them were involved in the glyceride metabolism pathway, and the distribution of most of them in brain at 24 hpf then in liver and intestine at 96 hpf suggested their potential roles in lipid and glyceride metabolism to apply energy for normal development in zebrafish.

Lipids are hydrophobic molecules, including phospholipids, glycolipids, cholesterol, triglycerides, and fatty acids, which are important components of cell membranes (Kao et al. 2020). Cu is an important trace element in the body, mainly distributed in the liver, blood, intestines, and other tissues, and Cu overload

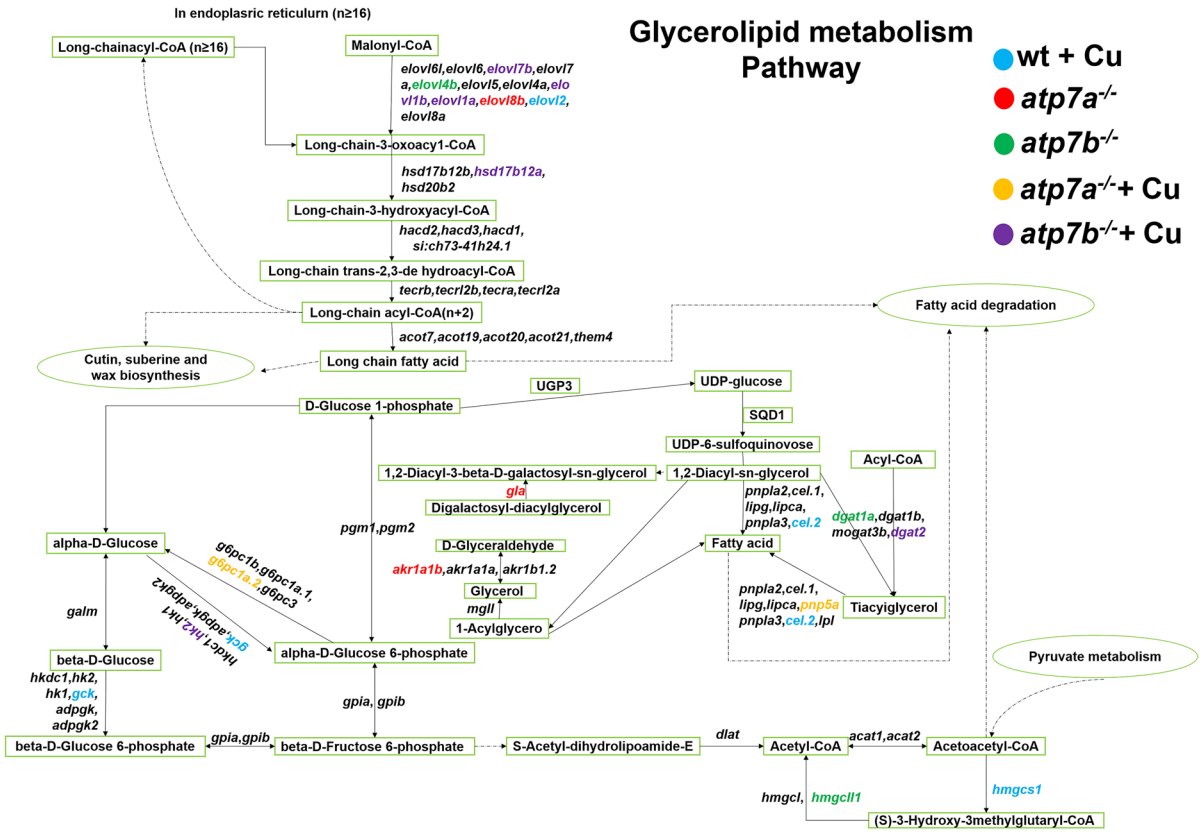

Fig. 6 The correlation between lipid metabolism-related DEGs of WT + Cu, *atp7a*$^{-/-}$, *atp7b*$^{-/-}$, *atp7a*$^{-/-}$ + Cu, *atp7b*$^{-/-}$ + Cu was established by KEGG pathway analysis

will lead to abnormal development of the body and lipid metabolism disorders in fish livers (Chen et al. 2012; Mcgeer et al. 2000). Furthermore, in rats, Cu overload inhibits Cu–Zn superoxide dismutase (SOD) activity and leads to elevation of malondialdehyde (MDA) in serum and liver, resulting in lipid peroxidative damage (Zhang et al. 2000).

We have reported that Cu stress can lead to defects in intestinal development recently (Zhao et al. 2020b). In this study, based on aforementioned RNA-Seq data, we found that genes related to lipid metabolism processes, such as fatty acid metabolism and steroid biosynthesis, were all down-regulated in Cu-stressed larvae. Lipid metabolism is a complex physiological activity, and it has been shown that Cu overload was associated with dysfunctional cholesterol biosynthesis, dysfunctional synthesis of polyunsaturated fatty acid (PUFA), and glycolytic/gluconeogenesis enzymes such as HMG-COA (Gutiérrez-García et al. 2013). Consistently, in this study, it was unveiled that the gene mRNA transcription levels of enzyme 1 (*hmgcs1*), long-chain fatty acid elongase 2 (*elovl2*), glucokinase (*gck*), and carboxyester lipase 2 (*cel.2*) all changed to varying degrees in Cu-stressed embryos via RNA-Seq and the further qRT-PCR and WISH assays. Meanwhile, WISH assays unveiled spatiotemporally specific expression and distribution of the four genes during zebrafish embryogenesis, which were mainly concentrated in the head at 24 hpf and distributed in the liver and intestine at 96 hpf. The liver and intestine are the main sites of lipid metabolism in zebrafish (Joseph et al. 2003; Velagapudi et al. 2010), and the dynamic and spatiotemporal distribution of the four genes during embryogenesis further convinced their potential roles in lipid metabolism. Meanwhile, zebrafish embryos rely on the yolk nutrients which are mostly lipid, glycogen, and glycolipid (Sant and Timme-Laragy 2018), and the observations here that four genes are dominantly distributing in the brain at 24 hpf further suggested their potential roles in lipid and glycogen metabolism to apply energy for normal brain development in early zebrafish developmental stages.

HMGCS1 is the first rate-limiting enzyme in the HMG-CoA reductase–cholesterol synthesis pathway. Mutation or reduced expression of HMGCS1 will inhibit cholesterol synthesis (Fujimoto et al. 2021), and Cu overload alters cholesterol biosynthesis in hepatocytes, leading to a reduction in hepatic and serum cholesterol (Gutiérrez-García et al. 2013; Huster 2014). Consistently, the observations here that Cu stress induced changed expression of *hmgcs1* during zebrafish embryogenesis and GO term of cholesterol metabolism was enriched for the DEGs.

In addition, one of the functions of the liver is to maintain blood glucose concentrations within the physiological range. GCK is the first key rate-limiting enzyme in oxidative phosphorylation during glycolysis, catalyzing the conversion of glucose to glucose-6-phosphate, which reduces blood glucose levels by enhancing energy metabolism in the liver (Kishore et al. 2017; Porat et al. 2011). In the liver, simultaneous elevation of glucose concentration and insulin content enhances GCK activity and gene expression, alters its subcellular localization, and interacts with regulatory proteins to promote glycolysis and hepatic glycogen synthesis to meet the regulation of normal physiological activities (Baldini et al. 2016). This key enzymatic reaction determines the metabolism of glucose in the liver, including gluconeogenesis, glycolysis, lipogenesis, and glycogen synthesis. In the present study, *gck* gene expression was up-regulated after Cu stress in zebrafish, which may be a marker of enhanced oxidative stress in the liver caused by heavy metals. Similarly, in rats treated with nano-copper, it was found that the lactate level in the liver and kidney extracts significantly increased and the glucose content decreased (Lei et al. 2008), which is consistent with our results obtained in Cu-stressed zebrafish. This indicates that Cu overload may induce a large amount of glycolysis and anaerobic respiration to induce lactic acid accumulation by enhancing GCK activity, thereby causing liver toxicity and nephrotoxicity. Meanwhile, ELOVL2 is an elongase involved in the synthesis of long-chain polyunsaturated fatty acids and is mainly responsible for the endogenous synthesis of docosahexaenoic acid (DHA) in organisms (Liu et al. 2020; Pauter et al. 2014), inactivation of *elovl2* in zebrafish embryos not only interferes lipid synthesis and causes retinopathy (Chen et al. 2020; Dasyani et al. 2020), but also increases endoplasmic reticulum stress and mitochondrial dysfunction (Li et al. 2020). In this study, the expression of *elovl2* gene in zebrafish showed spatiotemporal specific expression in vivo, mainly concentrated in the head in 24 hpf embryos, but decreased in the brain in 96 hpf embryos, and gradually expressed in the liver and intestine, which was consistent with previous

studies related to *elovl2* expression in early developmental embryos of zebrafish (Monroig et al. 2009; Tan et al. 2010). Meanwhile, the reduced expression of *elovl2* was observed in Cu-stressed embryos at both 24 hpf and 96 hpf. We speculate that Cu overload led to the down-regulation of *elovl2* expression, which in turn affects polyunsaturated fatty acid synthesis and induces abnormal brain neurodevelopment and lipid metabolism disorders.

ATP7A and ATP7B are important Cu transporters in organisms, and they function importantly in excreting excess intracellular Cu ions to extracellular in intestinal and liver cells, respectively (La Fontaine and Mercer 2007). In this study, *atp7a*$^{-/-}$ and *atp7b*$^{-/-}$ mutants were used to explore the relationship between Cu hemostasis and lipid metabolism during zebrafish embryogenesis. Lipid metabolism-related DEGs were unveiled in both *atp7a*$^{-/-}$ and *atp7b*$^{-/-}$ mutants, indicating that the loss of ATP7A and ATP7B function, respectively, both affects lipid metabolism during zebrafish embryogenesis. ATP7A is mainly responsible for the uptake of dietary Cu in the gut and for Cu transport in most cells, and ATP7B is mainly responsible for the transport and excretion of Cu in the liver (Linder et al. 1998). Menkes disease patients with ATP7A deficiency show large amounts of Cu ions accumulation in the gut (Ravia et al. 2005). Meanwhile, Wilson's disease patients with ATP7B deficiency show excess Cu accumulating in the brain and liver and develop cirrhosis and neurodegenerative diseases (Ala et al. 2007). In this study, genes such as *gla*, *gsr*, *st3gal5*, *elovl8b*, *akr1a1b*, *hmgcll1*, *elovl4b*, *lss*, *apoa4b.1*, and *dgat1a*, which function in lipid metabolism, exhibited significantly differential expressions in *atp7a*$^{-/-}$ and *atp7b*$^{-/-}$ mutants, respectively. We speculate that the differential induction of lipid metabolism occurred in *atp7a*$^{-/-}$ and *atp7b*$^{-/-}$ mutants might be caused by the Cu accumulation in gut and liver, respectively. The observations here are consistent with the studies that *Atp7a*$^{-/-}$ mice are lighter than normal mice with a significant down-regulation in fat content under high-fat diet (Yao and Qin 2015) and significant down-regulation of processes such as de novo lipid synthesis (DNL), cholesterol synthesis, and reduced lipid utilization with characteristics of hepatic lipidosis in *Atp7b*$^{-/-}$ mice (Tama et al. 2020).

To understand the roles of Cu transporters ATP7A and ATP7B in Cu-induced lipid metabolism defects during zebrafish embryogenesis, we further tested transcriptome profiles in *atp7a*$^{-/-}$ and *atp7b*$^{-/-}$ mutants with and without Cu stress. GO analysis for DEGs showed that the lipid metabolism-related entries, such as adipocytokine signaling pathway and steroid hormone biosynthesis, were significantly enriched in *atp7a*$^{-/-}$ mutants after Cu stress, while the lipid metabolism-related entries, such as lipid transport and cholesterol homeostasis, were significantly enriched in *atp7b*$^{-/-}$ mutants after Cu stress. In addition, we found that the expression levels of genes *hmgcs1* and *gck* did not change significantly in the *atp7a*$^{-/-}$ mutants after Cu stresses but significant changes occurred in Cu-stressed WT, which indicated that Cu stress affects the expression of *hmgcs1* and *gck* dependent on the integrate function of ATP7A. Meanwhile, the expression of the gene gck was significantly down-regulated in the *atp7b*$^{-/-}$ mutant after Cu stress but significantly up-regulated in WTs after Cu stress, suggesting that ATP7B is very important for the response of *gck* to Cu stress. Meanwhile, *cel.2* and *elovl2* still exhibited further down-regulated expressions in both *atp7a*$^{-/-}$ and *atp7b*$^{-/-}$ mutants after Cu stresses. The observations here not only suggested that the deficiency of both *atp7a* and *atp7b* could not block Cu-induced abnormalities in some of lipid metabolism pathways during zebrafish embryogenesis, but also suggested that genes differential responding to Cu stress in *atp7a*$^{-/-}$ and *atp7b*$^{-/-}$ mutants might be potential lipid metabolism indicators in gut and liver, respectively, because the liver and intestine are the most important lipid metabolism organs in the body and Cu-stressed *atp7a*$^{-/-}$ and *atp7b*$^{-/-}$ mutants concentrated more Cu ions in gut and liver, respectively, as studies reported (Ackerman et al. 2018; Ala et al. 2007).

The systematic understanding of the DEGs in lipid metabolism unveiled that most of the lipid metabolism-related DEGs unveiled in this study were involved in part of the glycerolipid metabolism pathway, which was similar to the results of other reports (Pan et al. 2018) and similar to the report that heavy metal cadmium induced changes in the composition and co-metabolism of glycerolipids (Swa et al. 2021). The results of this study not only provide a theoretical basis for fish embryonic development and lipid metabolism disorders under Cu overload, but also provide possible new ideas for human metabolic

diseases such as ATP7A and ATP7B dysfunction and Cu homeostasis imbalance.

Author contribution C.S.L., Y.W., H.T.L.: methodology, investigation, formal analysis, data curation, visualization, writing—original draft. Y.W. and H.W. formulated the standard curve of Cu standard solution samples. Y.W.: writing—original draft, investigation, data analysis. J-X.L.: conceptualization, resources, funding acquisition, supervision, writing—review and editing.

Funding This work was finally supported by the Knowledge Innovation Program of Wuhan-Basic Research (2022020801010223), the National Key R&D Program of China (2018YFD0900101), the National Natural Science Foundation of China (Program No. 32070807 to J-X.L), and by the project 2020SKLBC-KF06 of State Key Laboratory of Biocontrol (to J-X.L.).

Data availability All data generated or analyzed during this study are included in this published article.

Declarations

Ethics approval All animals and experiments were conducted in accordance with the "Guidelines for Experimental Animals" approved by the Institutional Animal Care and Use Ethics Committee of Huazhong Agricultural University (HZAUFI-2016–007).

Conflict of interest The authors declare no competing interests.

References

Ackerman CM, Weber PK, Xiao T, Bao T, Kuo TJ, Zhang E, Jennifer PR, Chang CJ (2018) Multimodal LA-ICP-MS and nanoSIMS imaging enables copper mapping within photoreceptor megamitochondria in a zebrafish model of Menkes disease. Metallomics 10:474–485

Ala A, Walker AP, Ashkan K, Dooley JS, Schilsky ML (2007) Wilson's disease. Lancet 369:397–408

Antonio Guardiola F, Cuesta A, Meseguer J, Angeles Esteban M (2012) Risks of using antifouling biocides in aquaculture. Int J Mol Sci 13:1541–1560

Baldini SF, Steenackers A, Stichelen OV, Mir AM, Mortuaire M, Lefebvre T, Guinez C (2016) Glucokinase expression is regulated by glucose through O-GlcNAc glycosylation. Biochem Biophys Res Commun 478:942–948

Brewer GJ (2015) Copper-2 ingestion, plus increased meat eating leading to increased copper absorption, are major factors behind the current epidemic of Alzheimer's disease. Nutrients 7:10053–10064

Brewer GJ, Kanzer SH, Zimmerman EA, Celmins DF, Heckman SM, Dick R (2010) Copper and ceruloplasmin abnormalities in Alzheimer's disease. Ame J Alzheimers Dis and Other Dementias 25:490–497

Chen QL, Luo Z, Liu X, Song YF, Zhao YH (2012) Effects of waterborne chronic copper exposure on hepatic lipid metabolism and metal-element composition in Synechogobius hasta. Arch Environ Contam Toxicol 64:301–315

Chen MY, Luo Y, Xu JP, Chang MX, Liu JX (2019) Copper regulates the susceptibility of zebrafish larvae to inflammatory stimuli by controlling neutrophil/macrophage survival. Front Immunol 10:2599

Chen D, Chao DL, Rocha L, Kolar M, Nguyen Huu VA, Krawczyk M, Dasyani M, Wang T, Jafari M, Jabari M, Ross KD, Saghatelian A, Hamilton BA, Zhang K, Skowronska-Krawczyk D (2020) The lipid elongation enzyme ELOVL2 is a molecular regulator of aging in the retina. Aging Cell 19:e13100

Dasyani M, Gao F, Xu Q, Fossan DV, Chao DL (2020) Elovl2 is required for robust visual function in zebrafish. Cells 9:2583

Festa RA, Thiele DJ (2011) Copper: an essential metal in biology. Curr Biol 21:R877–R883

Fontaine SL, Mercer J (2007a) Trafficking of the copper-ATPases, ATP7A and ATP7B: role in copper homeostasis. Arch Biochem Biophys 463:149–167

Fortin C, Couillard Y, Campbell B (2010) Determination of free Cd, Cu and Zn concentrations in lake waters by in situ diffusion followed by column equilibration ion-exchange. Aquat Geochem 16:151–172

Fujimoto N, Akiyama M, Satoh Y, Tajima S (2021) Interaction of galectin-7 with HMGCS1 in vitro may facilitate cholesterol deposition in cultured keratinocytes. J Investig Dermatol 142:539–548

Gutiérrez-García R, Pozo TA, Suazo M, CambiazoGonzaLez VM (2013) Physiological copper exposure in Jurkat cells induces changes in the expression of genes encoding cholesterol biosynthesis proteins. Biometals 26:1033–1040

Halfdanarson TR, Kumar N, Hogan WJ, Murray JA (2009) Copper deficiency in celiac disease. J Clin Gastroenterol 43:162–164

Huster D (2014) Structural and metabolic changes in Atp7b−/− mouse liver and potential for new interventions in Wilson's disease. Ann N Y Acad Sci 1315:37–44

Joseph SB, Castrillo A, Laffitte BA, Mangelsdorf DJ, Tontonoz P (2003) Reciprocal regulation of inflammation and lipid metabolism by liver X receptors. Nat Med 9:213–219

Kao YC, Ho PC, Tu YK, Jou IM, Tsai KJ (2020) Lipids and Alzheimer's disease. Int J Mol Sci 21:1505

Kimmel CB, Ballard WW, Kimmel SR, Ullmann B, Schilling TF (1995) Stages of embryonic-development of the zebrafish. Dev Dyn 203:253–310

Kishore M, Cheung K, Fu H, Bonacina F, Wang G, Coe D, Ward EJ, Colamatteo A, Jangani M, Baragetti A (2017) Regulatory T cell migration is dependent on glucokinase-mediated glycolysis. Elsevier Sponsored Documents 47:831–832

Krishnamoorthy L, Cotruvo JA Jr, Chan J, Kaluarachchi H, Muchenditsi A, Pendyala VS, Jia S, Aron AT, Ackerman CM, Vander Wal MN, Guan T, Smaga LP, Farhi SL, New EJ, Lutsenko S, Chang CJ (2016) Copper regulates cyclic-AMP-dependent lipolysis. Nat Chem Biol 12:586–592

Lei R, Wu C, Yang B, Ma H, Shi C, Wang Q, Wang Q, Yuan Y, Liao M (2008) Integrated metabolomic analysis of

the nano-sized copper particle-induced hepatotoxicity and nephrotoxicity in rats: a rapid in vivo screening method for nanotoxicity. Toxicol Appl Pharmacol 232:292–301

Li X, Wang J, Wang L, Feng G, Zhang K (2020) Retraction for Li et al., Impaired lipid metabolism by age-dependent DNA methylation alterations accelerates aging. Proc Natl Acad Sci USA 117:8660

Linder MC, Wooten L, Cerveza P, Cotton S, Shulze R, Lomeli N (1998) Copper transport. Am J Clin Nutr 67:965S-971S

Liu JX, Zhang D, Xie X, Ouyang G, Liu X, Sun Y, Xiao W (2013) Eaf1 and Eaf2 negatively regulate canonical Wnt/beta-catenin signaling. Development 140:1067–1078

Liu C, Ye D, Wang H, He M, Sun Y (2020) Elovl2 but not Elovl5 is essential for the biosynthesis of docosahexaenoic acid (DHA) in zebrafish: insight from a comparative gene knockout study. Mar Biotechnol 22:613–619

Llanos RM, Mercer JFB (2002) The molecular basis of copper homeostasis and copper-related disorders. DNA Cell Biol 21:259–270

Loennerdal B (2008) Intestinal regulation of copper homeostasis: a developmental perspective. Am J Clin Nutr 88:846S-850S

Logan S, Agbaga MP, Chan M, Brush RS, Anderson RE (2014) Endoplasmic reticulum microenvironment and conserved histidines govern ELOVL4 fatty acid elongase activity. J Lipid Res 55(4):698–708

Makokha VA, Qi Y, Shen Y, Wang J (2016) Concentrations, distribution, and ecological risk assessment of heavy metals in the East Dongting and Honghu Lake, China. Exposure and Health 8:31–41

Mcgeer JC, Szebedinszky C, Mcdonald DG, Wood CM (2000) Effects of chronic sublethal exposure to waterborne Cu, Cd or Zn in rainbow trout 2: tissue specific metal accumulation. Aquat Toxicol 50:245–256

Mi X, Li Z, Yan J, Li Y, Zheng J, Zhuang Z, Yang W, Gong L, Shi J (2020) Activation of HIF-1 signaling ameliorates liver steatosis in zebrafish atp7b deficiency (Wilson's disease) models. Biochimica Et Biophysica Acta-Molecular Basis of Disease 1866(10):165842

Monroig Ó, Rotllant J, Sánchez E, Cerdá-Reverter J, Tocher DR (2009) Expression of long-chain polyunsaturated fatty acid (LC-PUFA) biosynthesis genes during zebrafish Danio rerio early embryogenesis. Bba Molecul & Cell Biol Lipids 1791:1093–1101

Morrell A, Tallino S, Yu L, Burkhead JL (2017) The role of insufficient copper in lipid synthesis and fatty-liver disease. IUBMB Life 69:263–270

Oehrvik H, Thiele DJ, New York Acad S (2014) How copper traverses cellular membranes through the mammalian copper transporter 1, Ctr1. Ann NY Acad Sci 1314:32–41

Pan YaXiong, Mei-Qing Z, Dan-Dan Li, Yi-Huan Xu, Kun Wu (2018) SREBP-1 and LXRα pathways mediated Cu-induced hepatic lipid metabolism in zebrafish Danio rerio. Chemosphere 215:370–379

Pauter AM, Olsson P, Asadi A, Herslof B, Jacobsson A (2014) Elovl2 ablation demonstrates that systemic DHA is endogenously produced and is essential for lipid homeostasis in mice. J Lipid Res 55:718–728

Pfeil SA, Lynn DJ (1999) Wilson's disease – copper unfettered. J Clin Gastroenterol 29:22–31

Porat S, Weinberg-Corem N, Tornovsky-Babaey S, Schyr-Ben-Haroush R, Hija A, Stolovich-Rain M, Dadon D, Granot Z, Ben-Hur V, White P (2011) Control of pancreatic β cell regeneration by glucose metabolism – ScienceDirect. Cell Metab 13:440–449

Ravia JJ, Stephen RM, Ghishan FK, Collins JF (2005) Menkes copper ATPase (Atp7a) is a novel metal-responsive gene in rat duodenum, and immunoreactive protein is present on brush-border and basolateral membrane domains. J Biol Chem 280:36221–36227

Sant KE, Timme-Laragy AR (2018) Zebrafish as a model for toxicological perturbation of yolk and nutrition in the early embryo. Current Environmental Health Reports 5(1):125–133

Sassa T, Ohno Y, Suzuki S, Nomura T, Nishioka C, Kashiwagi T, Hirayama T, Akiyama M, Taguchi R, Shimizu H (2013) Impaired epidermal permeability barrier in mice lacking Elovl1, the gene responsible for very-long-chain fatty acid production. Mol Cell Biol 33:2787–2796

Shan W, Xia X, Lin C, Xi C, Zhou C (2010) Levels of arsenic and heavy metals in the rural soils of Beijing and their changes over the last two decades (1985–2008). J Hazard Mater 179:860–868

Svensson PA, Englund MCO, Markstrom E, Ohlsson BG, Jernas M, Billig H, Torgerson JS, Wiklund O, Carlsson LMS, Carlsson B (2003) Copper induces the expression of cholesterogenic genes in human macrophages. Atherosclerosis 169:71–76

Swa B, Ch A, Xw C, Yw A, Min YD, Hx D, Ssd E, Kw A, Qt A, Sx F (2021) Cadmium-induced changes in composition and co-metabolism of glycerolipids species in wheat root: glycerolipidomic and transcriptomic approach. J Hazard Mater 423:5

Tai ZP, Guan PP, Wang ZY, Li LY, Zhang T, Li GL, Liu JX (2019) Common responses of fish embryos to metals: an integrated analysis of transcriptomes and methylomes in zebrafish embryos under the stress of copper ions or silver nanoparticles. Metallomics 9:9

Tama B, Nms C, Vm C (2020) Lipid and energy metabolism in Wilson disease. Liver Research 4:10

Tan SH, Chung HH, Shu-Chien AC (2010) Distinct developmental expression of two elongase family members in zebrafish. Biochem Biophys Res Commun 393:397–403

Tao C, Wang Y, Zhao Y, Pan J, Fan Y, Liang X, Cao C, Zhao J, Petris MJ, Li K, Wang Y (2019) Adipocyte-specific disruption of ATPase copper transporting alpha in mice accelerates lipoatrophy. Diabetologia 62:2340–2353

Velagapudi VR, Hezaveh R, Reigstad CS, Gopalacharyulu P, Yetukuri L, Islam S, Felin J, Perkins R, Boren J, Oresic M (2010) The gut microbiota modulates host energy and lipid metabolism in mice. J Lipid Res 51:1101–1112

Yao J, Qin Z (2015) Counteract of bone marrow of blotchy mice against the increases of plasma copper levels induced by high-fat diets in LDLR−/− mice. J Trace Elem Med Biol 31:11–17

Zhang SSZ, Noordin MM, Rahman SOA, Haron J (2000) Effects of copper overload on hepatic lipid peroxidation and antioxidant defense in rats. Vet Hum Toxicol 42:261–264

Zhang T, Xu L, Wu J-J, Wang W-M, Mei J, Ma X-F, Liu J-X (2015) Transcriptional responses and mechanisms of

copper-induced dysfunctional locomotor behavior in zebrafish embryos. Toxicol Sci 148:299–310

Zhang Y, Zhang R, Sun H, Chen Q, Yu X, Zhang T, Yi M, Liu J-X (2018) Copper inhibits hatching of fish embryos via inducing reactive oxygen species and down-regulating Wnt signaling. Aquat Toxicol 205:156–164

Zhang T, Guan P, Liu W, Zhao G, Fang Y, Fu H, Gui J-F, Li G, Liu J-X (2020) Copper stress induces zebrafish central neural system myelin defects via WNT/NOTCH-hoxb5b signaling and pou3f1/fam168a/fam168b DNA methylation. Biochimica Et Biophys Acta-Gene Regul Mechan 1863:194612

Zhao G, Sun HJ, Zhang T, Liu JX (2020a) Copper induce zebrafish retinal developmental defects via triggering stresses and apoptosis. Cell Commun Signal 18:45

Zhao G, Zhang T, Sun H, Liu J-X (2020b) Copper nanoparticles induce zebrafish intestinal defects via endoplasmic reticulum and oxidative stress. Metallomics 12:12–22